

Supersymmetry and Future Colliders ¹

M. M. Nojiri

YITP, Kyoto University, Kyoto, 606-8502

E-mail: nojiri@yukawa.kyoto-u.ac.jp

Abstract

In this talk, I review precision SUSY study at LHC and TeV scale e^+e^- linear colliders (LC). We discuss the study of the 3 body decay $\tilde{\chi}_2^0 \rightarrow \tilde{\chi}_1^0 ll$ or the 2 body decay $\tilde{\chi}_2^0 \rightarrow \tilde{l}l$ at LHC. In the former case, the whole m_{ll} distribution observed at LHC would constrain ino mixing and slepton masses. On the other hand, when $\tilde{l}l$ decay is open, the distribution of the asymmetry of the transverse momentum of lepton pair $A_T = p_{T1}/p_{T2}$ peaks at $A_E = p_1/p_2$ at χ_2^0 rest frame for $m_{ll} \ll m_{ll}^{\max}$ samples, providing another model independent information. The peak position and the edge of the m_{ll} distribution constrain $m_{\tilde{\chi}_2^0}$, $m_{\tilde{\chi}_1^0}$ and $m_{\tilde{l}}$. Slepton mass universality may be checked within a few % in the early stage of experiment. Finally I discuss the physics at TeV scale LC. The mass and couplings of sparticles will be measured within $O(1\%)$ error, and measurement of the radiative correction to the ino-slepton-lepton coupling will determine the first generation squark mass scale even in decoupling scenarios.

¹ Talk given in International Symposium on Supersymmetry, Sugergravity, and Superstring(SSS99), Seoul, Korea, June 23(Wed)-27(Sun), 1999. Part of this talk is based on the project in progress with D. Toya and T. Kobayashi, ICEPP, Tokyo University.

1 Introduction

The Minimal Supersymmetric Standard Model (MSSM) is one of the promising extension of Standard Model. If the nature picks up the low energy supersymmetry(SUSY), MSSM will be proven *for sure*, as superpartners will be copiously produced at future colliders such as Large Hadron Collider (LHC) at CERN or TeV scale e^+e^- linear colliders (LC) proposed by DESY, KEK, and SLAC. The symmetry also offers natural solution of the hierarchy problem, amazing gauge coupling unification, and dark matter candidates.

On the other hand, the MSSM suffers sever flavor changing neutral current (FCNC) constraints if no mass relation is imposed on sfermion mass parameters. Various proposals have been made of the mechanism to incorporate the SUSY breaking to “our sector”, trying to offer the natural explanation of such mass relations. In short, it would be very surprising if sparticles are found in any future collider— The discovery is not the goal, but it is the beginning of a new quest of “the mechanism” of SUSY breaking. Measurements of soft breaking masses would be an important aspects of the SUSY study at future colliders, because different SUSY breaking mechanism predict different sparticle mass patterns.

In this talk, I will review attempts to measure soft breaking parameters at LHC and LC’s. In section 2 and 3, I will concentrate on the process that \tilde{g} and \tilde{q} are produced and decay, involving the leptonic second lightest neutralino decay $\tilde{\chi}_2^0 \rightarrow \chi_1^0 l^+ l^-$. The decay either proceeds through virtual exchanges of Z^0 and l or direct two body decays such as $\tilde{\chi}_2^0 \rightarrow \tilde{l} l$ and $\tilde{l} \rightarrow l \tilde{\chi}_1^0$. Events near the end point of the m_{ll} distribution of the three body decay play a key role to reconstruct the kinematics of \tilde{g} and \tilde{q} cascade decay chain, and minimal supergravity parameters is determined precisely.[1] In section 3.1, I point out the three body decay distribution depends strongly on the decay matrix element. This dependence may reduce the m_{ll} end point resolution, while the whole shape of m_{ll} distribution could provide information on slepton masses and ino mixings.[2] I also show a new analysis for the case where $\tilde{\chi}_2^0$ decays dominantly into $\tilde{l} l$. [3] We point out that the peak position of p_T asymmetry of the same flavor opposite sign (OS) lepton pairs in $m_{ll} \ll m_{ll}^{max}$ region would be independent of $\tilde{\chi}_2^0$ momentum distribution, therefore may be used to constraint $m_{\tilde{\chi}_2^0}$, $m_{\tilde{\chi}_1^0}$ and $m_{\tilde{l}}$ directly such as the end point of the m_{ll} distribution.

In section 4, I discuss precision study at future LC’s. Thanks to low backgrounds at polarized e^+e^- collider, the machine is perfect to discover and study the superparticles if they are in kinematical reach. Furthermore it

offers clean tests of relations of soft mass parameters and couplings. I discuss the radiative correction to the SUSY coupling relations which can be probed precisely at LC. The measurement of the deviation from the SUSY tree level relation offers a way to determine the squark mass scale in the “decoupling scenario”. [4]

2 Supersymmetry and LHC

Squarks (\tilde{q}) and gluinos (\tilde{g}) will be copiously produced at LHC, and they subsequently decay into charginos ($\tilde{\chi}_i^\pm$) or neutralinos ($\tilde{\chi}_i^0$). They could further decay into sleptons (\tilde{l}). The signal of the sparticle production will be leptons and/or jets with missing p_T if LSP is stable*. Various study indicates that LHC will find the excess of the sparticle signal if $m_{\tilde{q}}, m_{\tilde{g}} < 2$ TeV in MSUGRA scenarios.

The question is then if we could understand the nature of sparticles in detail. MSSM contains many parameters, on the other hand, the observed signal distributions are sum of products of production cross sections, branching ratios, and acceptances. The substantial complexities may prevent simple and model independent interpretations.

However some kinematical quantity can be extracted model independently by investigating some characteristic decay distributions. One of impressive examples is the case studied for Snowmass '96, so called “LHC point 3”. It is a case that the production of gluino followed by $\tilde{g} \rightarrow \tilde{b}b$, $\tilde{b} \rightarrow b\tilde{\chi}_2^0$ occurs with substantial branching fraction. The leptonic decay of the second lightest neutralino $\tilde{\chi}_2^0 \rightarrow \tilde{\chi}_1^0 l^+ l^-$ occurs with branching fraction of 16%. The number of $\tilde{b}\tilde{b}\tilde{b}l^+l^- + 2$ jet events then would be around 2.3 M for one year low luminosity run with S/N ratio about 10:1; This is substantially larger production ratio compared to typical s-channel sparticle production at LC. The end point of m_{ll} distribution of OS dileptons would be identified as $m_{\tilde{\chi}_2^0} - m_{\tilde{\chi}_1^0}$. The end point could be measured within 50 MeV error.

For point 3, $O(10^5)$ events near the m_{ll} end point could be selected for further analysis. In the limit where $m_{ll} \sim m_{ll}^{\max}$, $\tilde{\chi}_1^0$ is stopped in the rest frame of $\tilde{\chi}_2^0$, therefore $\vec{\beta}_{\tilde{\chi}_2^0} \propto \vec{\beta}_{\tilde{\chi}_1^0}$ in the laboratory frame. Assuming further an approximate MSUGRA relation $m_{\tilde{\chi}_2^0} = 2m_{\tilde{\chi}_1^0}$, one would reconstruct $m_{\tilde{l}}$ and $m_{\tilde{g}}$ through the invariant mass distribution of all possible combination of bottom jets and $\tilde{\chi}_2^0$ momentum. This leads to the resolution of MSUGRA parameters $m_0 = 200_{-8}^{+13}$ GeV and $M = 100 \pm 0.7$ GeV.

*I will concentrate on the MSUGRA motivated scenario where $\tilde{\chi}_1^0$ is the LSP.

The above analysis shows that the event distribution (which in principle depends on hundreds of parameters of MSSM model) could be factorized into a few distributions which sensitively reflect a few parameters of the model. The rest of the distributions will be understood better with the constraints. To this end, we may be able to provide enough cross checks between events and theoretical calculations (or MC simulations), so that we would be able to use event rates and whole distributions to determine model parameters precisely, or even reject some SUSY breaking scenarios.

3 Neutralino decay into leptons

In the previous section, we find the invariant mass distribution of OS lepton pairs from $\tilde{\chi}_2^0$ decay is the important part of the analysis. In this section we concentrate on some new aspects on the nature of the decay distribution and discuss the constraints to MSSM parameters that would be obtained from the distribution measurement.

3.1 Three body decay into $\tilde{\chi}_1^0 l^- l^+$ and the decay matrix element

Three body decays of $\tilde{\chi}_2^0$ are dominant as long as two body decays such as $\tilde{\chi}_2^0 \rightarrow \tilde{\chi}_1^0 Z^0$, $\tilde{\chi}_1^0 H$, $\tilde{\chi}_2^0 \rightarrow \tilde{l} l$ are not open. The branching ratio of the three body leptonic decay of the second lightest neutralino, $\tilde{\chi}_2^0 \rightarrow \tilde{\chi}_1^0 l^+ l^-$, is known to be very sensitive to the values of the underlying MSSM parameters. The dependence is enhanced by the negative interference between the decay amplitude from Z^0 exchange and that from slepton exchange. In this subsection we show that the effect of the interference appears not only in the branching ratios, but also in the decay distributions, such as the distribution of the invariant mass m_{ll} of the lepton pairs.

The partial decay width is given by

$$\frac{d\Gamma}{dx dy}(\tilde{\chi}_A^0 \rightarrow \tilde{\chi}_B^0 \bar{f} f) = \frac{N_C}{256\pi^3} m_{\tilde{\chi}_A^0} |\mathcal{M}|^2(x, y, z = 1 + r_{\tilde{\chi}_B}^2 - x - y). \quad (1)$$

The range of (x, y) is given by the conditions

$$\begin{aligned} z(xy - r_{\tilde{\chi}_B}^2) &\geq 0, \\ r_{\tilde{\chi}_B}^2 &\leq x \leq 1, \\ r_{\tilde{\chi}_B}^2 &\leq y \leq 1, \\ x + y + z &= 1 + r_{\tilde{\chi}_B}^2, \end{aligned} \quad (2)$$

when $m_f = 0$.

In the phase space of the decay $\tilde{\chi}_2^0 \rightarrow \tilde{\chi}_1^0 l^+ l^-$, the Z^0 exchange amplitude and \tilde{l} exchange amplitude behave differently. When the Z^0 contribution dominates, distributions are enhanced in the region of large $m_{\tilde{l}}^2 = z m_{\tilde{\chi}_2^0}^2$. In contrast, when the \tilde{l} exchange contribution dominates, distributions are enhanced in regions with large x and/or large y , therefore in small $m_{\tilde{l}}$ and large $|E_{l^-}^{\text{rest}} - E_{l^+}^{\text{rest}}|$ region. Note that $E_{l^+}^{\text{rest}} = (1-x)m_{\tilde{\chi}_2^0}/2$ and $E_{l^-}^{\text{rest}} = (1-y)m_{\tilde{\chi}_2^0}/2$ are lepton energies in the $\tilde{\chi}_2^0$ rest frame.

We consider the case where $2M_1 \sim M_2 \ll |\mu|$, a typical case in MSUGRA model. In this case, $\tilde{\chi}_2^0$ is Wino-like and $\tilde{\chi}_1^0$ is Bino-like. An interesting property in this case is that the Z^0 and \tilde{l} amplitudes could be of comparable size in some region of phase space. Furthermore, their interference is generally destructive for leptonic decays. These effects cause complicated situations, which we discuss below.

For illustration, we use two sets of parameters for the neutralino sector, (A) and (B), shown in Table 1. These values are fixed to give the same masses

set	M_1	M_2	μ	$\tan \beta$
(A)	70	140	-300	4
(B)	77.6	165	286	4

Table 1: Parameter sets for neutralinos. All entries with mass units are in GeV.

for three inos, $(m_{\tilde{\chi}_1^0}, m_{\tilde{\chi}_2^0}, m_{\tilde{\chi}_2^+}) = (71.4, 140.1, 320.6)$ GeV. For calculating the branching ratios, we take generation-independent slepton masses and a universal soft SUSY breaking squark mass $m_{\tilde{Q}} = 500$ GeV.

In Fig. 1a, we show the $m_{\tilde{l}}$ distribution of the decay $\tilde{\chi}_2^0 \rightarrow l^+ l^- \tilde{\chi}_1^0$ for parameter set (A) and varying $m_{\tilde{l}}$ from 170 GeV to 500 GeV. Because $m_{\tilde{\chi}_2^0}$ and $m_{\tilde{\chi}_1^0}$ are fixed, the end points of the distributions $m_{\tilde{l}}^{\text{max}} = 68.7$ GeV are same for each curve, while the shape of the distribution changes drastically with slepton mass. For a slepton mass of 170 GeV (thick solid line), the decay proceeds dominantly through slepton exchanges, therefore the $m_{\tilde{l}}$ distribution is suppressed near $m_{\tilde{l}}^{\text{max}}$. On the other hand, once slepton exchange is suppressed by its mass, Z^0 exchange dominates and the distribution peaks sharply near $m_{\tilde{l}}^{\text{max}}$.

In Fig. 1b, we show an example for $\mu > 0$, parameter set (B). The dependence on the slepton mass is different from the previous case. As $m_{\tilde{l}}$

increases from 170 GeV, m_{ll} distribution becomes softer. For $m_{\tilde{l}} > 250$ GeV, a second peak appears due to strong cancellation of Z^0 exchange and slepton exchange contributions for a certain value of m_{ll} . At the same time, the branching ratio reaches its minimum at $m_{\tilde{l}} \sim 300$ GeV, much less than 1%.

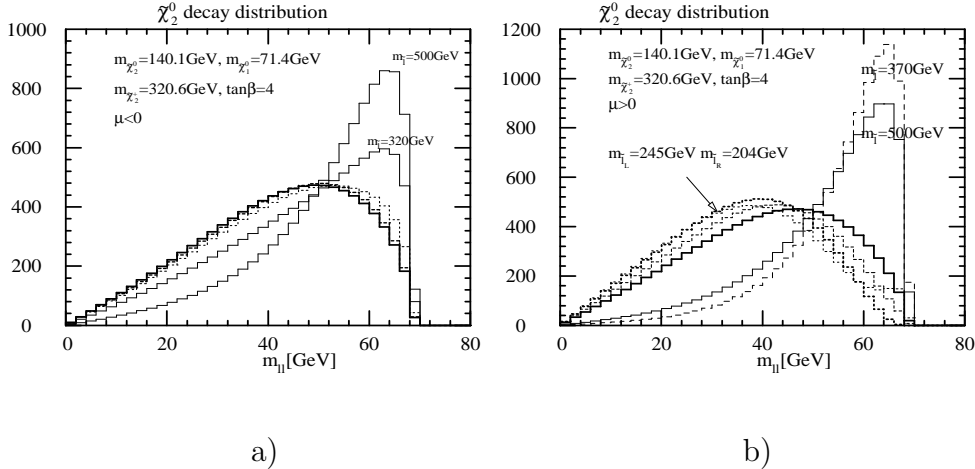


Figure 1: m_{ll} distribution of $\tilde{\chi}_2^0 \rightarrow \tilde{\chi}_1^0 ll$ decay for different $m_{\tilde{l}}$. a) $\mu < 0$, and b) $\mu > 0$. $m_{\tilde{\chi}_2^0} - m_{\tilde{\chi}_1^0}$ is fixed throughout the plots.

Notably, one can find slepton masses where a complete cancellation occurs very close to the end point m_{ll}^{\max} of the m_{ll} distribution. The thick dashed line shows distribution for $m_{\tilde{l}_L} = 245$ GeV and $m_{\tilde{l}_R} = 204$ GeV. Events near the end point ($m_{ll}^{\max} - m_{ll} < 4$ GeV) becomes too few, and it is very hard to observe the real end point for this case.

As it has discussed already, the lepton invariant mass distribution is an important tool for studying MSSM at hadron colliders. In previous studies, the end point of m_{ll} distribution is treated as ambiguous measurement of $m_{\tilde{\chi}_2^0} - m_{\tilde{\chi}_1^0}$, and the end point samples are used for further analysis. The slepton mass dependence of $\tilde{\chi}_2^0$ decay distribution shown in Fig. 1 suggests that not only the end point of the distributions but also the distributions themselves contain information about the underlying parameters such as $m_{\tilde{l}}$. The negative side of this is that the fitted end point may depend on the assumed values of these parameters, introducing additional systematic errors to the fit. For an extreme case shown in Fig. 2, the observed end point of the lepton invariant mass distribution does *not* coincide with $m_{\tilde{\chi}_2^0} - m_{\tilde{\chi}_1^0}$. Note that realistic simulations including the parameter dependence of the decay distribution were not available for hadron colliders until recently. The most recent ISAJET release (>ISAJET 7.43) allows to simulate the effect of exact

matrix elements for all three body decay distributions.

The m_{ll} distribution may be used to extract the underlying MSSM parameters. The distribution depends strongly on $m_{\tilde{l}}$, and also on $\tilde{\chi}_2^0 l \tilde{l}$ and $\tilde{\chi}_2^0 \tilde{\chi}_1^0 Z^0$ couplings. The Z^0 coupling is proportional to the Higgsino components of $\tilde{\chi}_2^0$ and $\tilde{\chi}_1^0$. Because we take these neutralinos to be gaugino-like, their Higgsino components depends on $\tan \beta$ and the Higgsino mass parameter μ , and $|\mu|$ is roughly equal to $m_{\tilde{\chi}_2^+}$. Therefore the m_{ll} distribution gives at least one constraint on μ , $\tan \beta$ and $m_{\tilde{l}}$ in addition to the well known constraint on $m_{\tilde{\chi}_2^0} - m_{\tilde{\chi}_1^0}$.

We estimate the sensitivity, assuming that backgrounds can be neglected or subtracted, and dependence of acceptance on m_{ll} can be corrected. We define the sensitivity function \mathcal{S} as follows:

$$\mathcal{S} = \sqrt{\sum_i \left(n_i^{\text{fit}} - n_i^{\text{input}} \right)^2 / n_i^{\text{input}}}. \quad (3)$$

Here n_i^{fit} (n_i^{input}) is the number of events in the i -th bin of the m_{ll} distribution for the MSSM parameters $(M_1, M_2, \mu, \tan \beta, m_{\tilde{l}_{L,R}})|_{\text{fit(input)}}$. We normalize $\sum_i n_i^{\text{fit}}$ and $\sum_i n_i^{\text{input}}$ to some number N . \mathcal{S} gives the deviation of the input distribution n_i^{input} from the distribution for the fit (n_i^{fit}) in units of standard deviations. We take $N = 2500$ and an m_{ll} bin size of 2 GeV.

In Fig. 2, we show contours of constant $\mathcal{S} = 1, 2, 3, 4$ (corresponding to $1\sigma, 2\sigma, 3\sigma, 4\sigma$ for $N=2500$) in the $(\tan \beta^{\text{fit}}, m_{\tilde{l}}^{\text{fit}})$ plane. For the solid lines, we take parameter set (A) and $m_{\tilde{l}} = 250$ GeV as input parameters, while for fitting parameters we vary $\tan \beta$ and $m_{\tilde{l}_L} = m_{\tilde{l}_R}$, fixing $(M_1^{\text{fit}}, M_2^{\text{fit}}, \mu^{\text{fit}})$ to reproduce the input values of $(m_{\tilde{\chi}_1^0}, m_{\tilde{\chi}_2^0}, m_{\tilde{\chi}_2^+})$. The resulting contours (solid lines) correspond to the sensitivity of the m_{ll} distribution to $m_{\tilde{l}}$ and $\tan \beta$ when the three ino masses are known.

In the figure, a strong upper bound on the slepton masses emerges, $m_{\tilde{l}} < 260$ GeV is obtained if $\mathcal{S} < 1$ is required. This is consistent with the large change of the distribution between $m_{\tilde{l}} = 270$ GeV and $m_{\tilde{l}} = 500$ GeV found in Fig. 1. The m_{ll} distribution also constrains $\tan \beta$ mildly. The constraint is not very strong due to our choice of parameters $|\mu| \gg M_2$; gaugino-Higgsino mixing is suppressed in this case.

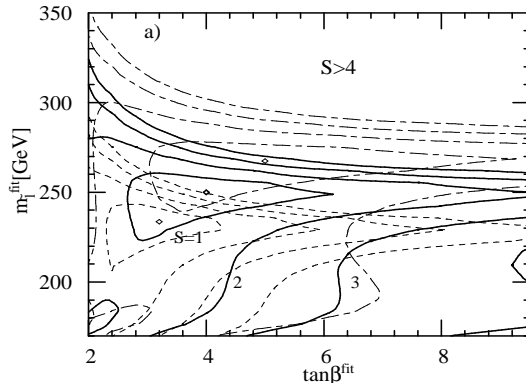


Figure 2: Constraint on $m_{\tilde{l}}$ and $\tan\beta$ from the m_{ll} distribution. Input parameters are set (A) with $m_{\tilde{l}} = 250$ GeV. For solid lines, we fix $m_{\tilde{\chi}_2^0}$, $m_{\tilde{\chi}_1^0}$ and $m_{\tilde{\chi}_2^+}$ equal to those for parameter set (A), while $\tan\beta^{\text{fit}}$ and $m_{\tilde{l}}^{\text{fit}}$ are varied to see the sensitivity of the $\tilde{\chi}_2^0$ decay distribution to these parameters. For the dot-dashed (dashed) lines, $m_{\tilde{\chi}_2^+}^{\text{fit}} = m_{\tilde{\chi}_2^+}^{\text{input}} + (-)30$ GeV.

3.2 The two body decay into $\tilde{l}\tilde{l}$ and lepton p_T asymmetry

We now discuss the case where $m_{\tilde{\chi}_2^0} > m_{\tilde{l}}$. The decay could proceed through two body decays

$$\tilde{\chi}_2^0 \rightarrow \tilde{l}^+ l^-, \tilde{l}^- l^+, \quad (4)$$

$$\tilde{l} \rightarrow \tilde{\chi}_1^0 l. \quad (5)$$

Because of the phase space factor, the decay could dominate over the three body decay $\tilde{\chi}_2^0 \rightarrow \tilde{\chi}_1^0 f \bar{f}$.

Note that the decay distribution is now completely fixed by the two body kinematics. The m_{ll} distribution of the two leptons from the $\tilde{\chi}_2^0$ cascade decay is

$$\frac{1}{\Gamma} \frac{d\Gamma}{dm_{ll}} = \frac{2m_{ll}}{(m_{ll}^{\text{max}})^2}. \quad (6)$$

Here the end point of the m_{ll} distribution, m_{ll}^{max} , is expressed as

$$m_{ll}^{\text{max}} = \frac{\sqrt{(m_{\tilde{\chi}_2^0}^2 - m_{\tilde{l}}^2)(m_{\tilde{l}}^2 - m_{\tilde{\chi}_1^0}^2)}}{m_{\tilde{l}}}. \quad (7)$$

In addition to that, it has been known that the the lepton p_T asymmetry $A_T (\equiv p_{T2}/p_{T1})$ distribution (where $p_{T1} > p_{T2}$) is sensitive to slepton

masses.[1, 5] The A_T can distribute off from 1 when it originates from $\tilde{\chi}_2^0$ and sometimes strongly peaks. (On the other hand, A_T distribution of the three body decay peaks at 1.) The asymmetry comes from the monochromatic nature of lepton energy from the $\tilde{\chi}_2^0$ decay in the rest frame. For example, when the mass difference between $\tilde{\chi}_2^0$ and \tilde{l} is small, the lepton energy from the $\tilde{\chi}_2^0$ decay is substantially smaller than that from \tilde{l} decay. The nature of the lepton p_T asymmetry is then qualitatively understand, because the lepton with high (low) energy in the $\tilde{\chi}_2^0$ rest frame has better chance to get high (low) p_T in the laboratory frame.

The purpose of this subsection is to improve this qualitative nature to quantitative one. We note that two leptons go exactly the same direction if $m_{ll} = 0$. In the limit, the ratio of the energies of the lepton antilepton pair is unchanged even if $\tilde{\chi}_2^0$ is boosted; A_T at $m_{ll} = 0$, A_T^0 , would be estimated by the lepton energy ratio $A_E(\equiv E_{l2}/E_{l1})$ at the $\tilde{\chi}_2^0$ rest frame at $m_{ll} = 0$, A_E^0 , as,

$$\begin{aligned}
A_T^0 \sim A_E^0 \equiv E_{l2}/E_{l1}|_{m_{ll} \sim 0} &= \frac{m_{\tilde{l}}^2 - m_{\tilde{\chi}_1^0}^2}{m_{\tilde{\chi}_2^0}^2 - m_{\tilde{l}}^2}, \quad (\text{for } m_{\tilde{l}}^2 - m_{\tilde{\chi}_1^0}^2 < m_{\tilde{\chi}_2^0}^2 - m_{\tilde{l}}^2) \\
\text{or} &\frac{m_{\tilde{\chi}_2^0}^2 - m_{\tilde{l}}^2}{m_{\tilde{l}}^2 - m_{\tilde{\chi}_1^0}^2} \quad (\text{for } m_{\tilde{l}}^2 - m_{\tilde{\chi}_1^0}^2 > m_{\tilde{\chi}_2^0}^2 - m_{\tilde{l}}^2).
\end{aligned} \tag{8}$$

Even though $m_{ll} \neq 0$, we see that distribution peaks at the same value; $A_T^{\text{peak}} = A_E^0$ holds approximately. In Fig 3, we show A_T distributions with various invariant mass cuts. Here we take the universal scalar mass $m = 100$ GeV, the universal gaugino mass $M = 150$ GeV, $\tan\beta = 2$, $A = 0$, and $\mu < 0$, when $m_{\tilde{e}_R} = 120.68$ GeV, $m_{\tilde{\chi}_1^0} = 65.15$ GeV and $m_{\tilde{\chi}_2^0} = 135.49$ GeV. The peak structure is quite prominent even without m_{ll} cuts. The edge of the m_{ll} decay distribution is 52 GeV.[†]

We can see that the peak solely comes from $m_{ll} \ll m_{ll}^{\text{max}}$ events. When we compare the distribution of the events with $m_{ll}^2 < 100$ (GeV)² (Fig.3 a) and $m_{ll}^2 < 400$ (GeV)² (Fig.3 b), we found that the event distribution is more sharply peaked at the value close to $A_E^0 = 0.368$ as m_{ll} cut decreases. The result of non-symmetric Gaussian fit to the events near the peak for $\int \mathcal{L} dt = 2.4 fb^{-1}$ is summarized in the table 1. The sample for $m_{ll} < 10$ GeV is in perfect agreement with the expected value A_E .

With sufficient statistics one may be able to measure the m_{ll} dependence of A_T in $m_{ll} \ll m_{ll}^{\text{max}}$ region. The lepton energy ratio for generic m_{ll} would

[†]The MSSM parameters and cuts are same to that is taken by Iashvili and Khar-chilava[5]. We use ISAJET7.44 and ATLFast2.21 for simulations.

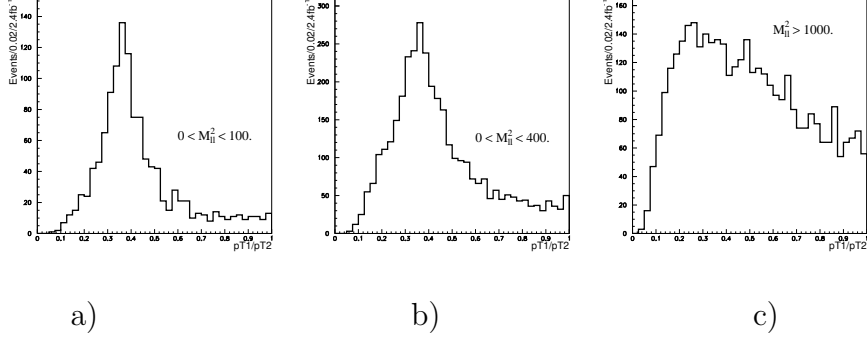


Figure 3: $A_T \equiv p_{T2}/p_{T1}$ distribution with different $m_{\tilde{u}}$ cut. a) $m_{\tilde{u}}^2 < 100$ (GeV) 2 , b) $m_{\tilde{u}}^2 < 400$ (GeV) 2 , c) $m_{\tilde{u}}^2 > 1000$ (GeV) 2

be given as

$$\frac{E_{l2}}{E_{l1}} = \frac{m_{\tilde{\chi}_2^0}^2 - m_{\tilde{l}}^2}{m_{\tilde{l}}^2 - m_{\tilde{\chi}_1^0}^2 + 2m_{\tilde{u}}^2} \quad (\text{for } m_{\tilde{l}}^2 - m_{\tilde{\chi}_1^0}^2 + m_{\tilde{u}}^2 > m_{\tilde{\chi}_2^0}^2 - m_{\tilde{l}}^2)$$

or

$$\frac{m_{\tilde{l}}^2 - m_{\tilde{\chi}_1^0}^2 + m_{\tilde{u}}^2}{m_{\tilde{\chi}_2^0}^2 - m_{\tilde{l}}^2} \quad (\text{for } m_{\tilde{l}}^2 - m_{\tilde{\chi}_1^0}^2 + m_{\tilde{u}}^2 < m_{\tilde{\chi}_2^0}^2 - m_{\tilde{l}}^2). \quad (9)$$

According to Eq.(9), the measurement of $m_{\tilde{u}}$ dependence of the peak position could correspond to the measurement of $m_{\tilde{l}}^2 - m_{\tilde{\chi}_1^0}^2$.

In Table 2, the fitted peak value reduces as $m_{\tilde{u}}$ cut increases. This could be due to the reduction of average E_{l1}/E_{l2} in the $\tilde{\chi}_2^0$ rest frame. $A_E = 0.354$ at $m_{\tilde{u}} = 20$ GeV for the parameters we take. The average A_E between $m_{\tilde{u}} = 0$ and 20 GeV agrees with the peak value of A_T distribution, though the statistics of this simulation is not sufficient to claim the deviation of the peaks between $m_{\tilde{u}}^2 < 100$ (GeV) 2 and $m_{\tilde{u}}^2 < 400$ (GeV) 2 samples. On the other hand, $A_E = 0.2915$ at $m_{\tilde{u}} = m_{\tilde{u}}^{\max} = 52$ GeV. The average A_E between $m_{\tilde{u}} = 0$ to $m_{\tilde{u}} = m_{\tilde{u}}^{\max}$ is too small compared to the A_T^{peak} without $m_{\tilde{u}}$ cut. This is consistent with the fact that no peak structure is observed for $m_{\tilde{u}}^2 > 1000(\text{GeV})^2$ (Fig. 3c).

To see the importance of A_T measurement, we first show the expected constraint on $m_{\tilde{l}}$ and $m_{\tilde{\chi}_1^0}$ when $m_{\tilde{\chi}_2^0}$ is fixed, provided that A_T and $m_{\tilde{u}}^{\max}$ is measured with the error of 0.07 and 0.5 GeV respectively (Fig.4). The error on $m_{\tilde{l}}$ and $m_{\tilde{\chi}_1^0}$ could be of the order of 1%, consistent with the previous fits[5]. Note they did not identify the origin of the peak structure and used *whole* A_T distribution for the fit. The used distribution may depend on parent squark and gluino masses, while our fit relies solely on the peak position, or only on $m_{\tilde{\chi}_1^0}$, $m_{\tilde{\chi}_2^0}$ and $m_{\tilde{l}}$.

	$m_{ll}^2 < 100 \text{ (GeV)}^2$ $0.30 < A_T < 0.40$	$m_{ll} < 400 \text{ (GeV)}^2$ $0.20 < A_T < 0.40$	no m_{ll} cut $0.15 < A_T < 0.40$
peak value	0.362	0.352	0.349
Error	0.660×10^{-2}	0.637×10^{-2}	0.685×10^{-2}

Table 2: Peak position and its error in A_T distribution

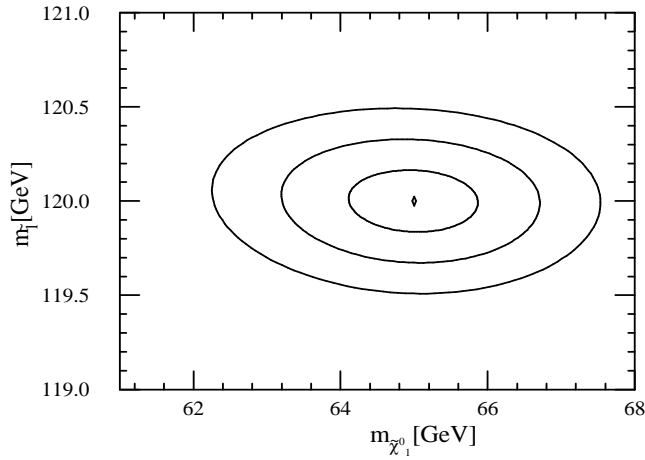


Figure 4: Contours of constant $\Delta\chi^2 = 1, 4, 9$ when $\delta A_T^{\text{peak}} < 0.07$ and $\delta m_{ll} = 0.5 \text{ GeV}$. $m_{\tilde{\chi}_2^0}$ is fixed for this fit.

One may also observe the end point of m_{ll} distribution of the three body decay in addition to the edge of the m_{ll} distribution originated from two body cascade decay through slepton. This is because right handed slepton coupling to wino and higgsino is zero. The measurements of m_{ll}^{max} (2 body), A_T^0 , and m_{ll}^{max} (3 body) $\equiv m_{\tilde{\chi}_2^0} - m_{\tilde{\chi}_1^0}$ are potentially sufficient to determine all sparticle masses involved in the $\tilde{\chi}_2^0$ cascade decay. Assuming a rather optimistic error on m_{ll}^{max} (3 body), $\delta m_{ll}^{\text{max}}$ (3 body) = 1 GeV, $m_{\tilde{\chi}_1^0}$, $m_{\tilde{\chi}_2^0}$, and $m_{\tilde{l}}$ are constrained within $\sim \pm 8 \text{ GeV}$, without assuming any relation between ino and slepton masses. The errors are substantially larger than those shown in Fig.4, due to the correlations between the constraints. On the other hand, $m_{\tilde{e}}/m_{\tilde{\mu}}$ ratio would be constrained strongly. Assuming $\delta A_T < 0.07$, $\delta m_{ee, \mu\mu} < 0.5 \text{ GeV}$, $\delta m_{ll}^{\text{max}}$ (3body) = 4 GeV, we obtain $\delta(m_{\tilde{e}}/m_{\tilde{\mu}}) = 2.5 \%$ for $\Delta\chi^2 < 1$, and 7% for $\Delta\chi^2 < 9$.

Note that the background in $m_{ll} \ll m_{ll}^{\text{max}}$ region must be studied to

claim the above measurement is possible. Backgrounds from $t\bar{t}\bar{l}$ could be important in low $m_{\tilde{u}}$ region. Note that the full amplitude level study of $W\gamma^*$ production has been done for the background process of $\tilde{\chi}_2^0 \tilde{\chi}_1^+ \rightarrow 3l$, and large background is found in $m_{\tilde{u}} < 10$ GeV region[6]. However it is unlikely that the background distribution has peak in $0 \ll A_T$ region. The peak of the signal distribution may be observed precisely on the top of such backgrounds, especially when signal rate is high enough to allow precision studies.

4 Precision study at LC

A TeV scale linear colliders could be a powerful discovery machine. In the context of MSUGRA model, 1 TeV LC roughly corresponds to LHC in its discovery potential. This is because that in the model with universal scalar and gaugino mass at very high scale, relations $m_{\tilde{Q}} \gg m_{\tilde{t}}$ and $m_{\tilde{g}} \gg m_{\tilde{W}}, m_{\tilde{B}}$ are predicted naturally. In future LC's, search modes are the production and the decay of sleptons, charginos, and neutralinos.

We should also note that LC experiments cover the case where superparticles takes nasty patterns of mass spectrum. Because of the available high beam polarization, backgrounds from W^\pm boson pair production can be highly suppressed. Notice also that its effective \sqrt{s} is monochromatic for e^+e^- colliders, therefore \tilde{l} and $\tilde{\chi}_1^+$ will be produced subsequently from lighter to heavier, and we can measure production cross sections and the decay distributions systematically.

Systematical studies of physics potential at LC when slepton, chargino and neutralino are produced have been done in detail by several authors[7], and it has been shown that gaugino mass relations, slepton mass relation, and coupling relations can be confirmed with errors of $O(1\%)$.

In this note, we concentrate on measurements of the coupling relations imposed by supersymmetry,

$$\begin{aligned} g_{\tilde{B}\tilde{e}_R e_R} &= \sqrt{2}g_B, \\ g_{\tilde{W}\tilde{e}_L e_L} &= \sqrt{2}g_W. \end{aligned} \tag{10}$$

It has been argued that this coupling relation could be measured within $O(1\%)$ accuracy or better by measuring sparticle production cross sections, angular distributions, and sparticle masses involved in the production process [4, 8].

The measurement of the couplings is important because the equivalence of the gauge coupling and gaugino coupling is ultimate probe of the supersymmetry at low energy, although the partial discovery of sparticle of course

suggests the existence. Another way to say, the existence of (large) SUSY breaking sector couples to (observed) sparticles will appear as the deviation of the sparticle coupling from those predicted by the tree level symmetry.

Such corrections might come from the existence of squarks which is much heavier than sleptons, charginos or neutralino. Such scenarios, with relatively light third generation squarks are occasionally quoted as “decoupling” scenarios, and attractive because they are free from large flavor changing neutral currents. When such mass spectrum is realized, SUSY coupling relations do not hold in the effective theory below $m_{\tilde{q}}$, and the corrections to the couplings from the tree level predictions are expressed as follows;

$$\begin{aligned}\delta\left(\frac{g_{\tilde{B}\tilde{e}e}}{g_{\tilde{B}}^{SM}}\right) &= 0.7\% \log_{10}\left(\frac{m_{\tilde{q}}}{m_{\tilde{l}}}\right), \\ \delta\left(\frac{g_{\tilde{W}\tilde{e}e}}{g_{\tilde{W}}^{SM}}\right) &= 2\% \log_{10}\left(\frac{m_{\tilde{q}}}{m_{\tilde{l}}}\right).\end{aligned}\tag{11}$$

If t -channel exchange of sparticles dominates over s -channel exchange of gauge bosons, the cross section can be proportional to the 4th power of the coupling, and the correction to the cross section could be around 8% when $m_{\tilde{q}} = 10m_{\tilde{l}}$ for sneutrino and wino productions. A specific example is considered for $\tilde{\nu}\tilde{\nu}^*$ production with charginos lighter than $\tilde{\nu}$ [8]. The production is dominated by t channel exchange of charginos, and involve the wino-sneutrino-electron coupling. For integrated luminosity around $100fb^{-1}$, the accepted number of events consisted with e^+e^- and some other jets or leptons activity exceeds more than 10^4 events. With suitable constraint to $\tan\beta$ and heavier ino masses, $\log_{10}(m_{\tilde{q}}/m_{\tilde{l}})$ would be constrained within 0.09 (statistics) \pm 0.08 (sneutrino mass error).[‡]

It would not be very surprising if $\mathcal{O}(10^6)$ sparticle events is accumulated in future, with sufficient understanding on underlying parameter of MSSM models. Note that different sparticles produced simultaneously, and the proposed TESLA integrated luminosity is as large as $1\text{ ab}^{-1} = 1000fb^{-1}$. Then Does this mean that the production cross sections are measured within $\mathcal{O}(0.1\%)$ accuracy; a few % measurement of the first generation squark masses without producing them?

Apparently, measuring the number of signal events is not equivalent to the measurement of the production cross section. Measured production cross

[‡] Here the error from sneutrino mass uncertainty is relatively large due to $\beta_{\tilde{\nu}}^3$ behavior of the cross section near the sneutrino production threshold. Chargino threshold production is proportional to $\beta_{\tilde{\chi}}$ and the error due to the mass uncertainty might be controlled better.

sections suffer various uncertainties, which is schematically given as

$$\begin{aligned} \frac{\delta\sigma}{\sigma} = & \frac{1}{\sqrt{N_{\text{accept}}}} \oplus \frac{\delta\sigma}{\delta M_i} \delta M_i \oplus \frac{\delta\sigma}{\delta m_i} \delta m_i \oplus \dots \\ & \oplus \text{luminosity error} \oplus \text{energy resolution} \oplus \text{QED, QCD corrections...} \end{aligned} \quad (12)$$

where N_{accept} may be expressed as

$$\begin{aligned} N_{\text{accept}} = & Br(\text{sparticle} \rightarrow \text{visible or clean mode}) \\ & \times (\text{acceptance}) \times \left(\int dt \mathcal{L} \sigma \right). \end{aligned} \quad (13)$$

The branching ratios may be around $(50\%)^2$ and the acceptance could be as high as 50 %. In the right hand side of equation (12), the first line contains errors of underlying MSSM parameters that could be negligible in the limit of infinite statistics. The second line contains machine dependent errors and potentially large and uncontrolled QED and QCD corrections. They must be very small if we want to extract $< 1\%$ deviation of cross section, and would require the huge efforts.

5 Conclusion

In this talk, I discussed a ‘‘precision’’ study of supersymmetry in future colliders, LHC and LC.

The motivation of the precision study is to explore the origin of supersymmetry breaking and mechanisms to bring it to our sector. The signature must appear on the sparticle mass patterns, and would be studied in detail in LHC and LC.

For LHC, charginos and neutralinos are produced as decay products of \tilde{g} and \tilde{q} , and the nature of weak interacting sparticles will be studied. In this talk, I discussed the decay of the second lightest neutralino. The leptonic decays of the second lightest neutralino $\tilde{\chi}_2^0$ could be studied even though one does not know the parent neutralino momentum. The m_{ll} distribution of the three body decay is sensitive to neutralino mixing and slepton masses. If systematical errors can be controlled, one may be able to constrain slepton masses. When the two body decay $\tilde{\chi}_2^0 \rightarrow \tilde{l}$ is open, one would measure the peak of lepton p_T asymmetry in $m_{ll} \ll m_{ll}^{\text{max}}$. in addition to the edge of m_{ll} distribution of the two body decay and occasionally the m_{ll} end point of the three body . The information constrain the parent and daughter neutralino and slepton masses rather stringently in model independent manner.

In LC, not only masses of sparticles, but production cross sections and sparticle decay distributions will be measured precisely. Underlying MSSM parameters, such as sparticle soft mass parameters, $\tan\beta$, gaugino-sfermion-fermion coupling would be measured within precision of $O(1\%)$ or less. In this talk, we discuss the determination of squark mass scale in the “decoupling scenario” where \tilde{q} is much heavier than \tilde{W} , \tilde{B} , and \tilde{l} . The squark mass maybe constrained within $O(10\%)$ through the measurement of the deviation of $\tilde{W}\tilde{U}$ coupling from its tree level value, g_2^{SM} .

References

- [1] I. Hinchliffe, F. E. Paige, M. D. Shapiro, J. Soderqvist, and W. Yao, Phys. Rev. D **55**, 5520 (1997).
- [2] M. M. Nojiri and Y. Yamada, Phys. Rev. **D60**, 015006 (1999).
- [3] D. Toya, T. Kobayashi, and M. M. Nojiri, work in progress.
- [4] M. M. Nojiri, K. Fujii, and T. Tsukamoto, Phys. Rev. D **54**, 6756 (1996); H.-C. Cheng, J. L. Feng, and N. Polonsky, Phys. Rev. D **56**, 6875 (1997); D **57**, 152 (1998); E. Katz, L. Randall, and S. Su, Nucl. Phys. B **536**, 3 (1999);
- [5] I. Iashvili and A. Kharchilava, Nucl. Phys. B **526**, 153 (1998).
- [6] H. Baer, M. Drees, F. Paige, P. Quintana and X. Tata, “Trilepton signal for supersymmetry at the Fermilab Tevatron revisited,” hep-ph/9906233.
- [7] T. Tsukamoto, K. Fujii, H. Murayama, M. Yamaguchi, and Y. Okada, Phys. Rev. D **51**, 3153 (1995); J. L. Feng, M. E. Peskin, H. Murayama, and X. Tata, Phys. Rev. D **52**, 1418 (1995); H. Baer, R. Munroe, and X. Tata, Phys. Rev. D **54**, 6735 (1996); D **56**, 4424(E) (1997), and M. M. Nojiri, K. Fujii, and T. Tukamoto[4].
- [8] M. M. Nojiri, D. M. Pierce, and Y. Yamada, Phys. Rev. D **57**, 1539 (1998); S. Kiyoura, M. M. Nojiri, D. M. Pierce, and Y. Yamada, Phys. Rev. D **58**, 075002 (1998).